Heat of hydration, bleeding, viscosity, setting of $Ca(OH)_2$-GGBS and MgO-GGBS grouts

Hua Yu[a], Yaolin Yi[a*], and Cise Unluer[a, b]

[a]School of Civil and Environmental Engineering, Nanyang Technological University, Singapore.

[b]James Watt School of Engineering, University of Glasgow, UK.

[*]Corresponding author. Email: yiyaolin@ntu.edu.sg

Abstract

Hydrated lime ($Ca(OH)_2$)- and reactive magnesia (MgO)-activated ground granulated blast-furnace slag (GGBS) have shown advantages in geotechnical applications compared with Portland cement (PC). To apply these two novel binders in slurry form to field applications, the properties of their grouts need to be investigated, which is the objective of this study. The heat of hydration, bleeding, viscosity, and setting behavior of $Ca(OH)_2$-GGBS and MgO-GGBS grouts were investigated and compared with PC and pure GGBS grouts in this study. All grouts indicated a decrease in bleeding and setting time, but an increase in viscosity with decreasing the water/cementitious material (W/C) ratio. Compared with the PC grout, the pure GGBS grout with the same water/binder ratio demonstrated higher bleeding and setting time, and lower heat rate and viscosity. Bleeding and setting time decreased and peak heat rate and viscosity increased with an increase in the activator ($Ca(OH)_2$ or MgO)/GGBS ratio within GGBS-based grouts. The peak heat rate in $Ca(OH)_2$-GGBS grouts was higher than that of pure GGBS or $Ca(OH)_2$ grout, indicating that $Ca(OH)_2$ was effective on activating hydration of GGBS. The peak heat rate in MgO-GGBS grouts was significantly lower than MgO grout and the heat rate was limited after 8 hours. The bleeding and setting times of MgO-GGBS grouts were significantly lower than those of $Ca(OH)_2$-GGBS grouts, which was primarily attributed to the hydration of MgO.

Keywords: GGBS, Grout, Heat of hydration, Bleeding, Viscosity, Setting time

1 Introduction

Grouting refers to the process of injecting pumpable materials (e.g., liquids and mixed suspensions) under pressure into various spaces by improving the physical and chemical properties to fulfill requirements of engineering applications [1]. Portland cement (PC) grout has been widely used in various geotechnical applications, such as jet grouting, deep mixing, and permeation grouting. However, from the perspective of environmental impact, the major issues associated with PC manufacture include high CO_2 emissions (0.90 ton CO_2/ton PC) and energy consumptions (5240 MJ/ton PC) [2, 3].

As an industrial by-product, ground granulated blast-furnace slag (GGBS) shows significant advantages in environmental impacts, including low CO_2 emissions (0.07 ton CO_2/ton GGBS) and energy consumptions (1300 MJ/ton GGBS) [4, 5]. Due to the low rate of hydration and strength development of GGBS, alkaline activators are used to accelerate the hydration [6]. For geotechnical applications, strong alkalis (e.g., NaOH) have issues on short setting time and risks of handling high pH material. Therefore, researchers have investigated activators based on alkaline earth metals, e.g., quick lime (CaO), hydrated lime ($Ca(OH)_2$), and reactive magnesia (MgO). Lime has been used in geotechnical applications for a long history, while the reactive MgO has emerged recently as a sustainable construction material. Yi et al. [7] have demonstrated that CaO and $Ca(OH)_2$ have similar activating efficacy, but $Ca(OH)_2$ is easier to store than CaO. However, $Mg(OH)_2$ has been proved to have significantly lower activating efficacy than reactive MgO [8]. Therefore, $Ca(OH)_2$ and MgO are more practical GGBS activators for field applications. The potential use of $Ca(OH)_2$-GGBS and MgO-GGBS in soil stabilization has been investigated from the perspective of compressive strength, resistance to sulfate attack, immobilization of heavy metals, mineralogy, and microstructure, demonstrating advantages compared with PC [7-14].

To apply the two binders including $Ca(OH)_2$-GGBS and MgO-GGBS in a slurry form to field applications, these engineering properties of new grouts should also be quantified and analyzed. According to the USACE engineer manual for grouting technology [1] and the European standard for jet grouting [15], bleeding, viscosity, and setting time are typically quantified for investigating engineering performance of

grouts. The aforementioned engineering properties are dominantly affected by the hydration reactions in an early period (less than 24 hours). Calorimetry, the measurement of heat of hydration, is commonly used to study the hydration reaction of cementitious materials. Considering the hydration involved multiple chemical reactions [16] can affect rheological and physical properties of cementitious materials grouts, it is worthwhile to investigate the effect of $Ca(OH)_2$ and MgO on the heat of hydration of activated GGBS grouts for facilitating the understanding of their bleeding, viscosity, and setting properties. Hence, this study evaluates properties, including heat of hydration, bleeding, viscosity, setting, and volume stability of $Ca(OH)_2$-GGBS and MgO-GGBS grouts compared with pure GGBS and PC grouts.

2 Materials and Methodology

2.1 Materials and mixture proportions

GGBS and PC were purchased from the Engro Co. Ltd., Singapore. $Ca(OH)_2$ and MgO were purchased from the Goldcrest Int. Pte. Ltd. in Singapore and Meishen Technology Co. Ltd. in China, respectively. The MgO produced at temperatures of 700-800°C had the reactivity of 46 s tested according to Shand [17]. The chemical composition of all raw materials was tested by X-ray fluorescence (XRF) spectrometer according to ASTM C114 [18] and the results are given in Table 1. The particle size distribution was tested based on laser diffraction analysis according to ISO 13320 [19] as shown in Fig. 1. The specific gravities of raw materials (Table 1) were measured with kerosene according to ASTM C188 [20]. In this study, the activators refer to $Ca(OH)_2$ or MgO, and the binders refer to PC, pure GGBS, $Ca(OH)_2$-GGBS, and MgO-GGBS. Activator ($Ca(OH)_2$ or MgO)/GGBS mass ratios of 0/1, 0.05/0.95, 0.1/0.9, and 0.2/0.8 were used for $Ca(OH)_2$-GGBS and MgO-GGBS [7].

Table 1. Chemical composition (by % weight) and specific gravity of raw materials.

Material	CaO	SiO_2	Al_2O_3	Fe_2O_3	SO_3	MgO	K_2O	TiO_2	MnO	Na_2O	LOI	Gs
GGBS	43.24	28.41	13.84	0.49	4.25	7.05	0.42	1.40	0.34	0.35	0.24	2.90
PC	62.13	20.77	3.66	2.93	1.76	4.11	0.35	0.69	0.06	0.37	3.16	3.15
$Ca(OH)_2$	68.80	0.18	0.12	0.17	0.73	2.40	0.01	-	0.03	-	27.55	2.24
MgO	0.5	-	-	0.03	0.60	89.50	-	-	-	-	7.65	3.58

Note: LOI = loss on ignition; Gs = specific gravity

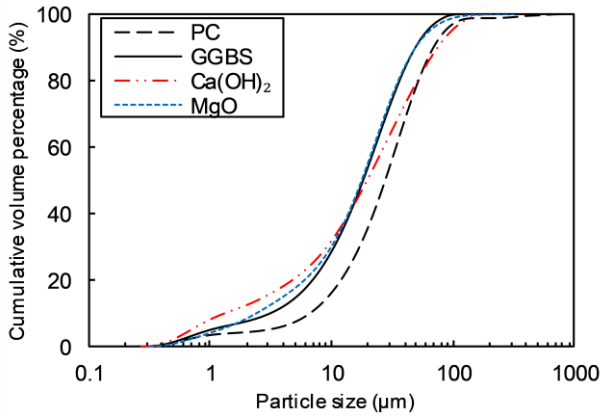

Fig. 1. Particle size distribution of PC, GGBS, $Ca(OH)_2$, and MgO.

Rosquoët et al. [21] summarized that the water/cementitious material (W/C) ratios of PC grouts were 0.3-1.5 for various applications including sealing grouts and injectable grouts for soils and rocks. USACE [1] indicates that the typical range for jet grouting is from 0.6 to 1.2, and the W/C ratio is designed as approximately 1.0 considering pumpability and engineering performance of grouts based on case studies and field tests [22, 23]. Therefore, considering early cement hydration generally decreases as W/C ratio increases [24], grouts with W/C ratio of 0.6 were tested for studying heat of hydration. Three W/C ratios of 0.8, 1.0, and 1.2 were designed in this study to evaluate the bleeding and viscosity of injectable grouts.

The setting time of grouts increases significantly with the increase of W/C ratio and final setting of PC grout with a W/C ratio of 0.7 is close to 12 hours [21]. Using a manual Vicat needle apparatus in this study, a long setting time can reduce the precision of results. Furthermore, for grouts with a high W/C ratio, the sample cannot be prepared as described in ASTM C191 [25] due to bleeding [26]. Previous researchers [27, 28] have used relatively low W/C ratios (≤ 0.4) for studying setting time of grouts. Hence, a low W/C ratio of 0.35 was used for the setting time measurement in this study.

2.2 Methodology

According to ASTM C1702 [29], the heat rates of grouts with the same W/C ratio of 0.6 were tested using a thermometric isothermal conduction calorimeter (Calmetrix I-Cal 8000 HPC). The weighted deionized water and dry activators or binders within plastic containers were initially stored in the

calorimeter with a constant temperature of 30℃ for 4 hours to reach the equilibrium state. The initial hydration rate of cementitious materials increases with increasing temperature [30]. The calorimeter temperature was set as 30°C because the ambient temperature of 23°C in laboratory would cause that the precipitation of hydrates proceeds slowly, especially for GGBS. After reaching the equilibrium state, water was added to the binders by manually mixing them with a plastic stick within 10 seconds. Then, the mixture was restored to the calorimeter for measuring the heat of hydration.

Bleeding was tested in accordance with ASTM C940 [31]. Referring to ASTM C940 [31], the bleeding (B) is defined as the ratio between the volume of bleed water above the suspension at the prescribed time interval (V_{wi}) and the total initial volume of the grout (V_o), i.e., $B = V_{wi}/V_o$. The final bleeding (FB) is defined as the ratio between the volume of decanted bleed water (V_w) and the volume of the total initial volume of the grout when there is no further expansion or bleeding (i.e., bleeding remains constant as the increase of time), i.e., $FB = V_w/V_o$.

Viscosity, as a measure of fluid's resistance to deformation due to internal molecule friction, is primarily used to evaluate the pumpability of grouts [32]. Marsh [33] initially introduced a test method to estimate the viscosity of fluids by using a funnel (i.e., Marsh viscosity, μ_M). This method shows great advantages in its simplicity and reliability under field conditions [34]. In this study, the viscosity of grouts was determined using the Marsh funnel according to ASTM D6910 [35]. GGBS and activator were initially mixed for five minutes by a laboratory mixer with 60 rpm. The amounts of water calculated based on W/C ratios were added to binders with mixing for another five minutes before conducting bleeding and viscosity tests.

The setting time test is used to determine the time of the skeletal structure of grout forms [21]. Appropriate setting time of grouts is important for engineering applications and both quick setting and slow setting may cause undesirable effects. According to ASTM C191 [25], both initial and final setting times of grouts were determined using a manual Vicat needle apparatus. The initial setting time is the time of Vicat needle penetration of 25 mm in the grout sample and final setting time is the time of first penetration

measurement without forming a complete circular impression mark on the specimen surface. The process of preparing samples took approximately one minute after initial contact of the binder with water.

The volume stability of hardened grouts was tested referring to ASTM C1090 [36]. All grouts were prepared with W/C ratio = 0.6, since a PC grout is typically prepared at W/C ratios ranging from 0.6 to 1.2 in jet grouting [1] and a higher W/C ratio may cause bias in measurement due to bleeding or drying effects [37]. After the initial curing of one day, the grout was placed under the micrometer bridge and vertical displacement was measured daily by a micrometer gauge. All tests in this study were performed in the laboratory with a temperature of ~23°C.

3 Results and Analysis

3.1 Heat of hydration

As shown in Fig. 2a, the typical curve with two peaks in heat rate of PC grout is observed: the first peak generally attributed to initial hydration of tricalcium silicate (C_3S) and formation of ettringite and the second peak due to hydration of C_3S to calcium silicate hydrate (CSH) [16, 38]. The heat rate of the second peak was higher than that of the first peak in PC grout. A possible reason is that the relatively high temperature of 30°C contributes to the acceleration of silicate reaction in the second peak [30]. A small initial peak was observed in pure GGBS grout, which is attributed to the wetting and dissolution of GGBS particles and adsorption of some ions onto the surface of GGBS particles [39]. The MgO grout also exhibited a single peak in the curve of heat rate with reaching the maximum value of 25 mW/g at 0.95 hours, which was significantly higher than the peak values of PC and pure GGBS grouts. The value of peak heat rate at 1.3 hours in the $Ca(OH)_2$ grouts was very low (< 0.5 mW/g). Although the dissolution of $Ca(OH)_2$ in water absorbs heat [40], the limited heat rate was observed in $Ca(OH)_2$ grouts, which should be attributed to a few percentages of CaO (or other materials reacting with water) in the hydrated lime.

Fig. 2b shows the effect of $Ca(OH)_2$ content on heat rate of $Ca(OH)_2$GGBS grouts. At the hydration time of 3.2 hours, the curves of $Ca(OH)_2$-GGBS grouts simultaneously reached the initial peaks. The peak

heat rate increased from 0.23 to 0.69 mW/g as the $Ca(OH)_2$/GGBS ratio increased from 0.05/0.95 to 0.2/0.8, which can be explained by the acceleration of the initial hydration of GGBS as activator content increases [38]. As the hydration time increased from 3 to 24 hours, the heat rate of $Ca(OH)_2$-GGBS grouts was significantly higher than that of pure GGBS or $Ca(OH)_2$ grouts, indicating the significant effect of $Ca(OH)_2$ on activating hydration reactions in GGBS. The heat rate increased for grouts with $Ca(OH)_2$/GGBS = 0.1/0.9 and 0.05/0.95 with reaching the second peaks at ~19.2 hours. A similar curve with two peaks in GGBS grouts activated by NaOH and Na_2SiO_3 was also observed in a past study [39]. The first peak is attributed to the wetting and dissolution of GGBS in an alkaline environment and the initial high pH of activator solution (i.e., high $Ca(OH)_2$ content) contributes to dissolve the GGBS for the formation of Ca-compounds [39]. The second peak is due to the formation of CSH caused by the reaction between the precipitated silicate ions and Ca^{2+} [39]. The peak of $Ca(OH)_2$-GGBS grouts is higher than that of pure GGBS or $Ca(OH)_2$, which indicates that $Ca(OH)_2$ is effective in activating hydration reaction in GGBS.

Fig. 2c shows the effect of MgO content on heat rate of MgO-GGBS grouts. Generally, as MgO/GGBS ratio increased from 0.05/0.95 to 0.2/0.8, the peak heat rate of grout increased from 0.89 to 1.73 mW/g, which was higher than that of pure GGBS grout with 0.32 mW/g. Compared with $Ca(OH)_2$-GGBS grouts, a single peak was observed in all MgO-GGBS gouts. The peaks reached at 0.72 hours for the grout with MgO/GGBS = 0.05/0.95 and at 1.2 hours for the grouts with MgO/GGBS = 0.1/0.9 and 0.2/0.8. The time reaching peaks of MgO-GGBS grouts was close to that of MgO grout (0.95 hours), indicating that the initial heat rate of MgO-GGBS grouts was primarily due to the hydration reaction of MgO. Unlike the $Ca(OH)_2$-GGBS grouts, regardless of MgO/GGBS ratio, only one peak was observed in MgO-GGBS grouts with heat rate less than 0.1 mW/g after 8 hours, indicating that MgO was less effective on activating hydration of GGBS in a period up to 24 hours. This result can be explained by the insufficient Ca^{2+} to form CSH that contributes to the second peak in MgO-GGBS grouts. It is worth noting that the comparison of activation between $Ca(OH)_2$-GGBS and MgO-GGBS grouts in this study is for the first 24

hours, while it may be different for a longer period. For example, previous studies [8, 10] indicated that MgO-GGBS could achieve higher strength than $Ca(OH)_2$-GGBS at 28 and 90 days.

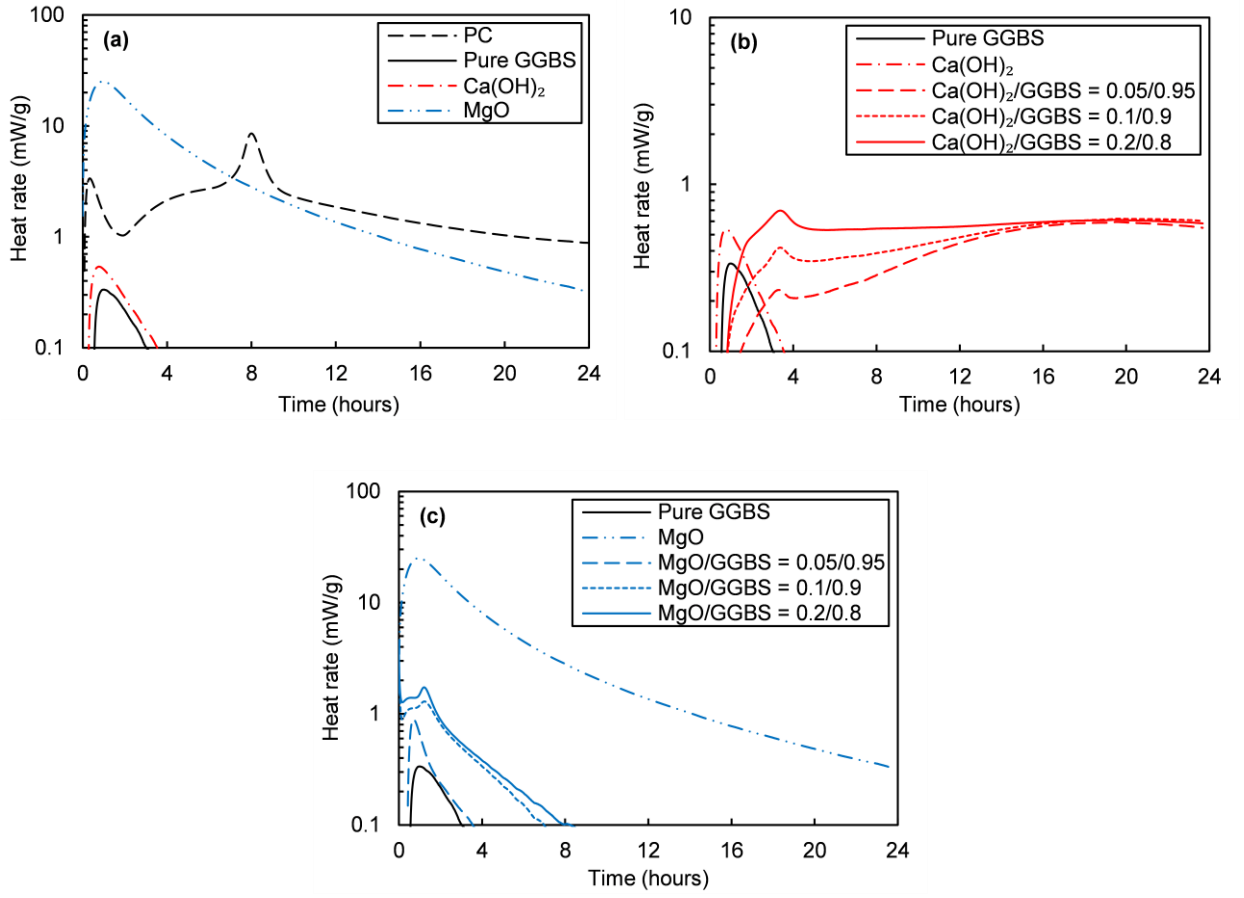

Fig. 2. Heat rate of (a) $Ca(OH)_2$ and MgO grouts, (b) $Ca(OH)_2$-GGBS grouts, and (c) MgO-GGBS grouts compared with PC and pure GGBS grouts.

3.2 Bleeding versus time

Fig. 3 shows the bleeding of different grouts versus time. Generally, all the grouts exhibited approximately linear bleeding-time curves after the initial mixing of the binders with water (≤ 60 mins), and the slopes of the curves decreased until the grouts reached the equilibrium state (i.e., the slope of the curve is zero). The time to reach the final bleeding (t_{FB}) for pure GGBS and $Ca(OH)_2$-GGBS grouts was higher than that of PC grout with the same W/C ratio. The effect of $Ca(OH)_2$ addition on t_{FB} of $Ca(OH)_2$-GGBS grouts was limited when the $Ca(OH)_2$/GGBS ratio increased from 0/1.0 (i.e., pure GGBS grout) to

0.2/0.8. However, the t_{FB} of MgO-GGBS grouts was much lower than that of PC grout with the same W/C ratio.

In bleeding tests, two competing forces including Brownian and gravitational forces are mainly considered for solid particles in a liquid medium. Some researchers [41, 42] used Stoke's theory to analyze the sedimentation of binder particles, according to which the settling velocity of the particle increases with increasing particle size and specific gravity. As shown in Fig. 2 and Table 1, both particle size and specific gravity of PC were higher than those of GGBS, which contributed to a higher settling velocity of the particles and reduced the t_{FB} in PC grouts as shown in Fig. 3. Compared with $Ca(OH)_2$-GGBS grouts, the lower values of t_{FB} of MgO-GGBS grouts can be attributed to that the MgO hydrates quickly and produces heat as shown in Fig. 2a, which reduces the W/C ratio in grouts and hence decreases the t_{FB}.

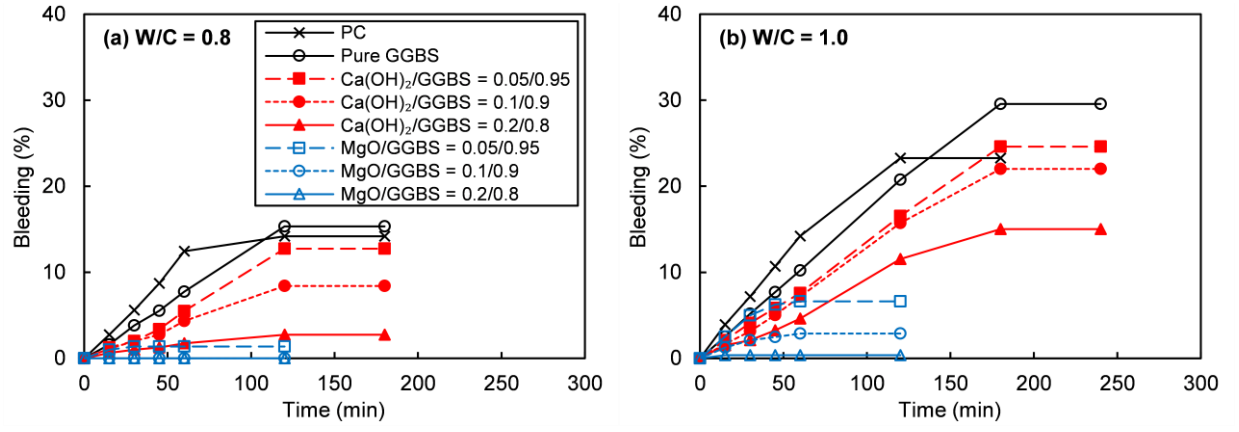

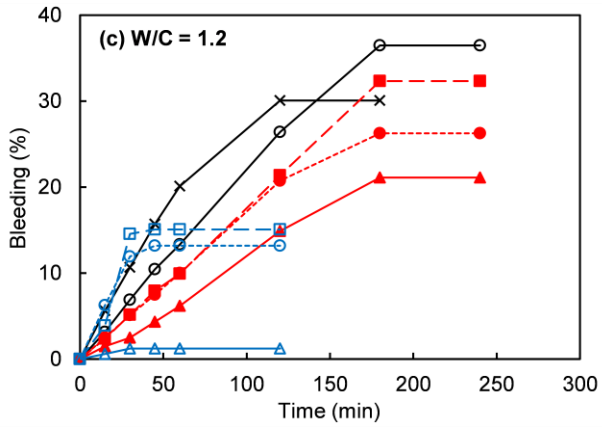

Fig. 3. Bleeding-time curves of PC and GGBS-based grouts: (a) W/C = 0.8, (b) W/C = 1.0, and (c) W/C = 1.2.

3.3 Final bleeding

Fig. 4 shows the final bleeding (FB) of PC and GGBS-based grouts. Generally, the FB of a grout increased with the increase of W/C ratio. The FB of pure GGBS grouts was significantly higher than that of PC grouts for W/C ratios of 1.0 and 1.2. By comparison, for W/C ratio = 0.8, the FB of pure GGBS was close to that of PC grout. For $Ca(OH)_2$-GGBS grouts, the FB decreased with the increase of $Ca(OH)_2$/GGBS ratio for each W/C ratio. The FB of MgO-GGBS grout was significantly lower than that of $Ca(OH)_2$-GGBS grout with the same W/C ratio and activator/GGBS ratio. For W/C ratio = 1.0 or 1.2, the FB of MgO-GGBS grout also decreased with the increase of MgO/GGBS ratio. As the W/C ratio decreased to 0.8, all FB values of MgO-GGBS grouts were close to zero. USACE [1] indicates that the ideal bleed for PC-based grout is zero because fractures or voids tend to remain filled during the injection of grouts in soils or rocks. However, from the perspective of practical uses, zero bleed is hard to reach with considering the pumpability of grouts. Therefore, a stable grout is generally characterized with 5% (or less) of FB [1, 15]. According to this criterion, none of the PC and pure GGBS grouts tested in this study is a stable grout. To reduce the bleeding water in grouts, methods of decreasing W/C ratio [43] or particle size of binder [26, 44] are suggested. For $Ca(OH)_2$-GGBS grouts, only the grout with $Ca(OH)_2$/GGBS = 0.2/0.8 and W/C ratio = 0.8 could be characterized as a stable grout. By comparison, most MgO-GGBS grouts (except the MgO/GGBS = 0.05/0.95 and 0.1/0/9 with W/C ratio = 1.2) were stable grouts.

The initial hydration rate of GGBS was slower than that of PC [39], which leads to the delay in the formation of hydration products (e.g., calcium-silicate-hydrate, C-S-H) that can physically restrict the movement of water to the surface of grout and then contribute an increase of FB [45]. For a fixed W/C ratio, the decreasing trend of FB with activator/GGBS ratio may be explained by the increase of hydration products in the grouts due to the positive correlation between the hydration rate of GGBS-based grouts and activator/GGBS ratio as shown in Figs. 2b and 2c. The FB of MgO-GGBS grout was significantly lower

than that of $Ca(OH)_2$-GGBS grout with the same W/C ratio and activator/GGBS ratio. This is because that MgO reacts with water to form magnesium hydroxide ($Mg(OH)_2$) and further reduces the W/C ratio besides the hydration reactions of activated GGBS, causing the decrease in distance of particles.

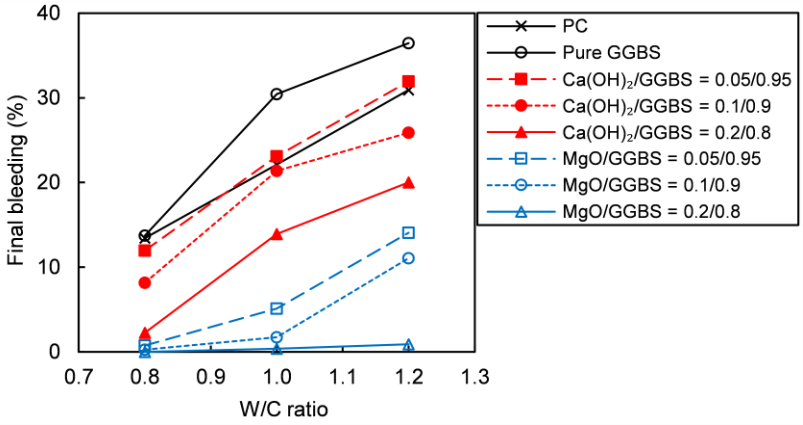

Fig. 4. Final bleeding of PC and GGBS-based grouts.

3.4 Marsh viscosity

Fig. 5 shows the Marsh viscosity, μ_M, for PC and GGBS-based grouts. Generally, the μ_M decreased with the increase of W/C ratio for all grouts. The μ_M of pure GGBS grout was slightly lower than that of PC grout with the same W/C ratio. For a fixed W/C ratio, the μ_M of GGBS-based grouts generally increased as the activator/GGBS ratio increased. This effect is more pronounced for the low W/C ratio of 0.8 and much less for W/C ratios of 1.0 and 1.2, at which the μ_M values of GGBS-based grouts with activator/GGBS ratios ranging from 0.05/0.95 to 0.1/0.9 are close to that of PC grout. For activator/GGBS = 0.2/0.8, the μ_M values of GGBS-based grouts were considerably higher than that of PC grout with the same W/C ratio. The μ_M values of all grouts, except the one with MgO/GGBS = 0.2/0.8 and W/C ratio = 0.8, were less than 60 s, which are groutable for moderate distance from the injection pump [46]. Typically, bleeding and viscosity are conflicting properties. For example, for all grouts, FB increased and μ_M decreased as W/C ratio increased, as shown in Figs. 3 and 4, respectively. The grouts with MgO/GGBS = 0.05/0.95 and 0.1/0.9 under W/C ratio = 1.0 show advantages considering both bleeding and viscosity properties, which are stable

with adding a small amount of MgO and also have similar μ_M values by comparing to PC grout with the same W/C ratio.

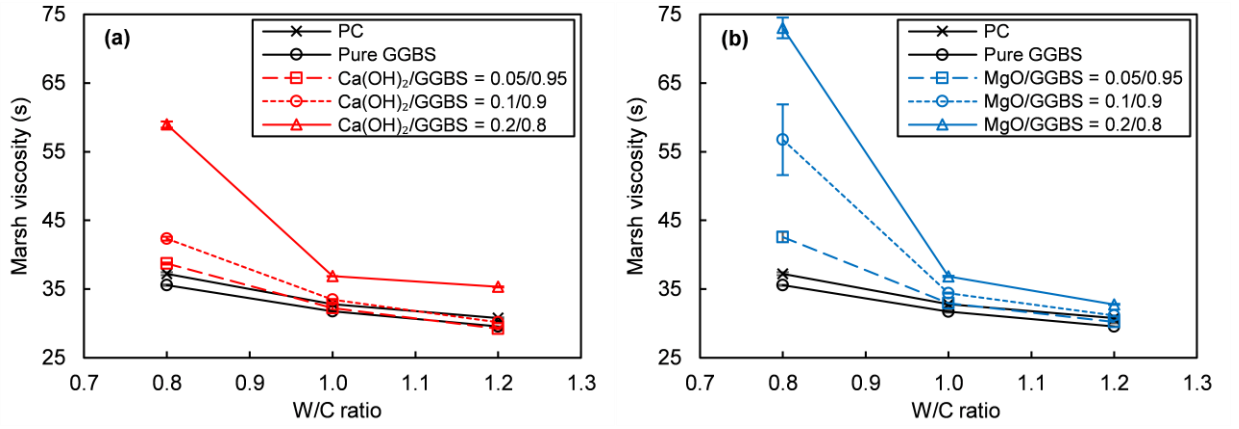

Fig. 5. Marsh viscosity of (a) $Ca(OH)_2$-GGBS grouts and (b) MgO-GGBS grouts compared with PC and pure GGBS grouts.

Marsh funnel tests for each grout mixture were performed three times consecutively (i.e., Tests 1-3) as three replicate tests. The time interval of two successive replicate tests was ~2 mins. For all PC and $Ca(OH)_2$-GGBS grouts, as well as MgO-GGBS grouts with W/C ratios = 1.0 and 1.2, the standard deviation of three replicate tests was low (< 0.5 s), which indicates that the viscosity of grouts can be considered as constant during the short testing period (< 5 mins). By comparison, as shown in Fig. 6, for MgO-GGBS grouts with W/C ratio = 0.8, μ_M increased significantly with the increase of elapsed time. In other words, the effect of time for conducting three replicate tests on the viscosity of MgO-GGBS grouts with a low W/C ratio is not negligible. In a short period, the significant increase in viscosity of MgO-GGBS with W/C ratio = 0.8 can be explained by the hydration of MgO and relatively small particle distance in grouts with low W/C ratio.

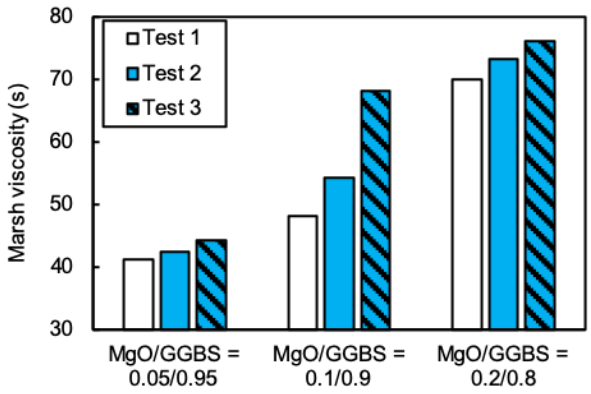

Fig. 6. Marsh viscosity tests for MgO-GGBS grouts with W/C = 0.8.

3.5 Setting time

The values of setting time of PC and GGBS-based grouts are summarized in Table 2. Both initial and final setting times of pure GGBS grout were significantly higher than those of PC grout. With the addition of activator, for $Ca(OH)_2$/GGBS ratios of 0.05/0.95 and 0.1/0.9, setting times of $Ca(OH)_2$-GGBS grouts were still higher than those of PC grout. As $Ca(OH)_2$/GGBS ratio increased to 0.2/0.8, setting times of $Ca(OH)_2$-GGBS grout were lower than those of PC grouts. Setting times of MgO-GGBS grout also decreased with increasing MgO/GGBS ratio, but they were all much lower than those of PC grout. The setting time of the grout with MgO/GGBS = 0.2/0.8 and W/C ratio = 0.35 was too quick to form into a ball required by ASTM C191 [25]. It is worth noting that, as W/C ratio increased to 0.4, setting times of MgO-GGBS grout were still significantly lower than those of $Ca(OH)_2$-GGBS grout (or PC grout) with a W/C ratio of 0.35.

Both initial and final setting times of pure GGBS grout were higher compared with PC grout, which agrees with previous studies [47, 48] that setting times of PC grout can be increased by adding GGBS. Brooks et al. [49] has indicated that the setting of PC is due to coagulation, which establishes contacts between cementitious grains, as well as the production of hydration products in the contact zones, which makes the coagulation structure rigid. Zhou et al. [47] further suggested that, compared with GGBS, PC particles pack more closely and yield greater inter-particle contact that can decrease setting times. The

decreasing trend in setting times with the increase of activator/GGBS ratio has been also observed in sodium silicate-activated GGBS-based grouts [50]. The setting times of MgO-GGBS grouts were significantly lower than $Ca(OH)_2$-GGBS grouts. A possible reason is that MgO not only accelerates the hydration reaction of GGBS-based grouts (as shown in Fig. 2c) but also further reduces the W/C ratio in grouts due to the MgO hydration.

Table 2. Initial and final setting time for different grouts.

Binder	PC	GGBS	$Ca(OH)_2$/GGBS			MgO/GGBS			
Ratio	-	-	0.05/0.95	0.1/0.9	0.2/0.8	0.05/0.95	0.1/0.9	0.2/0.8	0.2/0.8
W/C	0.35	0.35	0.35	0.35	0.35	0.35	0.35	0.35	0.4
Initial setting (min)	235	480	372	242	194	151	91	n/a	42
Final setting (min)	355	>540	535	490	300	235	220	n/a	140

Note: n/a = not applicable.

3.6 Volume stability

Fig. 7 shows the volume stability measuring the height change of hardened grouts with a W/C ratio of 0.6. As shown in Fig. 7, compared with PC grout, the GGBS grout exhibited volume shrinkage that was undesirable in grouting applications [1], which should be attributed to the slow hydration rate in GGBS (Fig. 2) and high bleeding (Fig. 3). For $Ca(OH)_2$-GGBS grouts, a general increasing trend in volume expansion was observed with increasing $Ca(OH)_2$ content. This is because $Ca(OH)_2$ accelerated the GGBS hydration and the formed hydration products contributed to the volume expansion of $Ca(OH)_2$-GGBS grouts. The expansive effect on grouts due to the growth of hydration products (e.g., ettringite) has been confirmed in previous studies [51, 52]. For MgO-GGBS grouts, the effect of MgO hydration on volume stability of grouts should be considered. The total volume of MgO and water can decrease up to 15% after hydration and formation of $Mg(OH)_2$. For a relatively low MgO content (MgO/GGBS $\leq$ 0.1/0.9), volume expansion was observed because MgO accelerated GGBS hydration and the formed hydration products contributed to the expansion, which could compensate for the volume decrease due to MgO hydration. However, as MgO/GGBS ratio increased to 0.2/0.8, a significant volume shrinkage was observed. For practical applications, $Ca(OH)_2$-GGBS and MgO-GGBS grouts with low MgO content exhibited slight

volume expansion, which were beneficial. However, the grout with MgO/GGBS = 0.2/0.8 is not recommended due to the volume shrinkage.

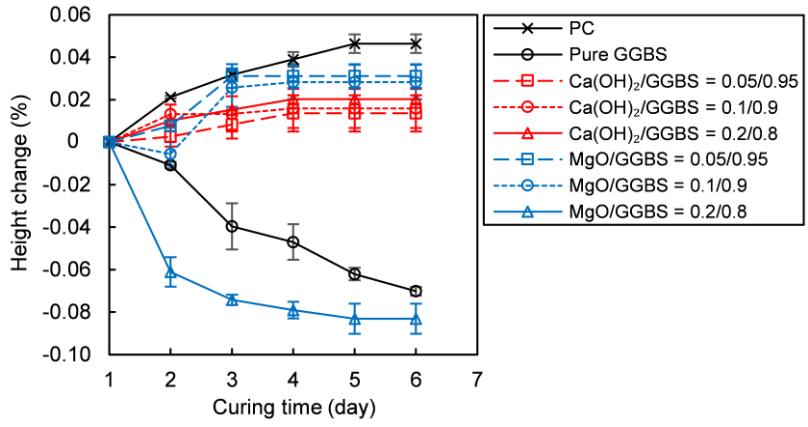

Fig. 7. Volume stability of PC and GGBS-based grouts.

Discussion

The selection of suitable grouting materials primarily depends on different practical applications. Based on laboratory-measured grout properties in this study, applications of GGBS-based grouts on jet grouting, wet deep mixing, and permeation grouting are discussed as below.

The jet grouting is used to mix and partially replace with soils by directly injecting high-velocity grouts, and the groutability for jet grouting is primarily evaluated based on the pumpability of grouts determined by the viscosity [53]. As W/C ratio increases, a grout tends to have low viscosity with the advantage of increasing the diameter of the jet-grouted column or reducing the required pump pressure. The wet deep mixing is another technique for soft ground improvement with the application of grouts. Compared with jet grouting, one major difference is that wet deep mixing relies on rotational mechanical mixing [54, 55]. Therefore, grouts with relatively high viscosity can be used because this application does not require to pump high-velocity grout. For W/C ratios of 1.0 and 1.2, $Ca(OH)_2$-GGBS and MgO-GGBS grouts had lower FB than PC grout without significantly increasing viscosity (Figs. 4 and 5). Compared with $Ca(OH)_2$-GGBS grouts, the setting times of MgO-GGBS grouts were significantly lower (Table 2), which negatively affects the pumpability (or groutability) in jet grouting. Therefore, for MgO-GBBS grouts,

a higher W/C ratio (≥ 1.0) is recommended in jet grouting with considering appropriate viscosity, bleeding, and setting times. For $Ca(OH)_2$-GGBS grouts, a low W/C ratio of 0.8 may be used in deep mixing and it is worth noting that grout with $Ca(OH)_2$/GGBS = 0.1/0.9 was close to a stable grout (8% of FB) with the limited increase in viscosity compared with PC grout, which may be beneficial for jet grouting and deep mixing.

The permeation grouting introduces grout into ground without disturbing the ground structure, and the groutability for permeation grouting is characterized as the ability of injection of grout into the soil or rock medium, which highlights the importance of the particle size characteristics of grouting materials [1, 56, 57]. Burwell [58] defined the groutability in soils (N_s) in terms of particle size as follows

$$N_{s1} = \frac{(D_{15})_{\text{soil}}}{(D_{85})_{\text{grout}}} \quad (1)$$

$$N_{s2} = \frac{(D_{10})_{\text{soil}}}{(D_{95})_{\text{grout}}} \quad (2)$$

where $(D_{10})_{soil}$ and $(D_{15})_{soil}$ are the particle sizes of soils corresponding to 10% and 15% finer, respectively. $(D_{85})_{grout}$ and $(D_{95})_{grout}$ are the particle sizes of grout material particles corresponding to 85% and 95% finer, respectively. Similarly, Mitchell [57] proposed the groutability in facture rock medium (N_r) with considering the relation between the width of rock fissure and diameter of the grout material particles. The higher N_r and N_s values indicate that the grouts can be more easily injected into the medium [57] and the increase of fineness of cementitious materials improves the groutability [59]. Compared with PC, GGBS and two activators have smaller particle sizes as shown in Fig. 1, which are beneficial to improve the groutability in permeation grouting. In field applications, besides the particle size distribution, other properties of grouts can also affect the groutability. The increase of viscosity in grout due to hydration reaction and decrease in porosity in the medium due to the infiltration phenomenon can reduce the groutability [60]. Compared with $Ca(OH)_2$-GGBS grouts, a significant increase in viscosity with increasing time was founded in MgO-GGBS grouts (Fig. 6), which could negatively affect the groutability in

permeation grouting. Although an increase in W/C ratio or grouting pressure is beneficial for improving groutability [61], grouts with high W/C ratios have disadvantages in the high mobility leading to flow significantly outside the treatment zone [1] and high FB exhibiting unstable grouts. Therefore, $Ca(OH)_2$-GGBS grouts with W/C ratio ≤ 1.0 were suggested to use in the permeation grouting due to the balance between viscosity and bleed. This study only investigated one type of MgO and one type of GGBS. It is known that the MgO reactivity and GGBS property can affect their performance of $Ca(OH)_2$-GGBS and MgO-GGBS grouts [13, 38, 62]. Hence, further studies are suggested to investigate the types of MgO and GGBS on the properties of MgO-GGBS grouts.

4 Conclusions

To apply two novel binders, $Ca(OH)_2$-GGBS and MgO-GGBS, in slurry form to field applications, this study investigated the properties of their grouts compared with PC and pure GGBS grouts. The main conclusions were drawn as follows:

1. The peak heat rate in $Ca(OH)_2$-GGBS grouts was higher than that of pure GGBS or $Ca(OH)_2$ grout, indicating that $Ca(OH)_2$ was effective on activating hydration of GGBS. A single peak of heat rate was observed in all MgO-GGBS grouts at a short time (< 1.5 hours) mainly due to hydration reaction in MgO. Compared with $Ca(OH)_2$, the heat rate in MgO-GGBS grouts was limited after 8 hours and the effect of MgO on accelerating GGBS hydration was relatively insignificant.

2. The time to reach the final bleeding (t_{FB}) of pure GGBS grout was higher than that of PC grout with the same W/C ratio. For a fixed W/C ratio, the t_{FB} of $Ca(OH)_2$-GGBS grouts were higher than that of PC grout, whilst the t_{FB} of MgO-GGBS grouts were lower than that of PC grout. Compared with $Ca(OH)_2$, MgO was more effective in reducing the final bleeding in GGBS-based grouts due to the hydration of MgO.

3. For a fixed W/C ratio, the Marsh viscosity, μ_M, of pure GGBS grout was lower than that of PC grout. As the activator/GGBS ratio increased, the μ_M increased significantly for GGBS-based grouts with

a low W/C ratio of 0.8. For W/C ratios of 1.0 and 1.2, the effect of activator/GGBS ratio on μ_M for GGBS-based grouts was relatively limited.

4. Both initial and final setting times of pure GGBS grout were longer than those of PC grout. Setting times of GGBS-based grouts decreased as the activator/GGBS ratio increased. MgO was more effective in reducing setting times of GGBS-based grouts compared with $Ca(OH)_2$ due to the hydration of MgO.

5. Compared with PC grout, pure GGBS grout had a disadvantage of volume shrinkage. As the $Ca(OH)_2$/GGBS ratio increased to 0.2/0.8 and MgO/GGBS ratio increased to 0.1/0.9, the engineering property of GGBS-based grouts had been improved by exhibiting the volume expansion. However, for grout with MgO/GGBS = 0.2/0.8, a significant volume shrinkage was observed mainly due to a large amount of water consumed by the hydration reaction in MgO.

Acknowledgments

The support from Nanyang Technological University (M4081914.030), Singapore, is appreciated.

References

[1] USACE, Engineering Manual for Grouting Technology, United States Army Corps of Engineers, Washington, D.C., 2017.

[2] WBCSD, Getting the Numbers Right (GNR) Project Reporting CO_2: Heat Consumption and Production, World Business Council for Sustainable Development (WBCSD), Geneva, 2016.

[3] R.M. Andrew, Global CO_2 emissions from cement production, 1928–2017, Earth Syst. Sci. Data 10(4) (2018) 2213-2239.

[4] M. Sumesh, U.J. Alengaram, M.Z. Jumaat, K.H. Mo, M.F. Alnahhal, Incorporation of nano-materials in cement composite and geopolymer based paste and mortar – A review, Constr. Build Mater. 148 (2017) 62-84.

[5] L.F. Cabeza, C. Barreneche, L. Miró, J.M. Morera, E. Bartolí, A. Inés Fernández, Low carbon and low embodied energy materials in buildings: A review, Renew. Sust. Energ. Rev. 23 (2013) 536-542.

[6] P. Mangat, P. Lambert, 18 - Sustainability of alkali-activated cementitious materials and geopolymers, in: J.M. Khatib (Ed.), Sustainability of Construction Materials (Second Edition), Woodhead Publishing, 2016, pp. 459-476.

[7] Y. Yi, L. Gu, S. Liu, Microstructural and mechanical properties of marine soft clay stabilized by lime-activated ground granulated blastfurnace slag, Appl. Clay Sci. 103 (2015) 71-76.

[8] Y. Yi, M. Liska, F. Jin, A. Al-Tabbaa, Mechanism of reactive magnesia – ground granulated blastfurnace slag (GGBS) soil stabilization, Can. Geotech. J. 53(5) (2015) 773-782.

[9] S. Wild, J.M. Kinuthia, R.B. Robinson, I. Humphreys, Effects of ground granulated blast furnace slag (GGBS) on the strength and swelling properties of lime-stabilized kaolinite in the presence of sulphates, Clay Miner. 31(3) (1996) 423-433.

[10] Y. Yi, M. Liska, A. Al-Tabbaa, Properties and microstructure of GGBS–magnesia pastes, Adv. Cem. Res. 26(2) (2014) 114-122.

[11] Y. Yi, X. Zheng, S. Liu, A. Al-Tabbaa, Comparison of reactive magnesia- and carbide slag-activated ground granulated blastfurnace slag and Portland cement for stabilisation of a natural soil, Appl. Clay Sci.111 (2015) 21-26.

[12] F. Jin, K. Gu, A. Al-Tabbaa, Strength and hydration properties of reactive MgO-activated ground granulated blastfurnace slag paste, Cem. Concr. Compos. 57 (2015) 8-16.

[13] F. Jin, K. Gu, A. Abdollahzadeh, A. Al-Tabbaa, Effects of Different Reactive MgOs on the Hydration of MgO-Activated GGBS Paste, J. Mater. Civil Eng. 27(7) (2015) B4014001.

[14] F. Jin, A. Al-Tabbaa, Evaluation of novel reactive MgO activated slag binder for the immobilisation of lead and zinc, Chemosphere 117 (2014) 285-294.

[15] EN, European Standard on the Execution of Special Geotechnical Works: Jet Grouting EN 12716, Brussels, Belgium, 2001.

[16] J.W. Bullard, H.M. Jennings, R.A. Livingston, A. Nonat, G.W. Scherer, J.S. Schweitzer, K.L. Scrivener, J.J. Thomas, Mechanisms of cement hydration, Cem. Concr. Res. 41(12) (2011) 1208-1223.

[17] M.A. Shand, The Chemistry and Technology of Magnesia, John Wiley & Sons, 2006.

[18] ASTM, Standard Test Methods for Chemical Analysis of Hydraulic Cement, ASTM C114, ASTM International, West Conshohocken, PA, 2018.

[19] ISO, Particle size analysis – Laser diffraction methods, ISO 13320, International Organization for Standardization, 2020.

[20] ASTM, Standard Test Method for Density of Hydraulic Cement, ASTM C188, ASTM International, West Conshohocken, PA, 2017.

[21] F. Rosquoët, A. Alexis, A. Khelidj, A. Phelipot, Experimental study of cement grout: Rheological behavior and sedimentation, Cem. Concr. Res. 33(5) (2003) 713-722.

[22] F.-H. Lee, Y. Lee, S.-H. Chew, K.-Y. Yong, Strength and Modulus of Marine Clay-Cement Mixes, J. Geotech. Geoenviron. Eng. 131(2) (2005) 178-186.

[23] S. Coulter, C.D. Martin, Effect of jet-grouting on surface settlements above the Aeschertunnel, Switzerland, Tunnelling and Underground Space Technology 21(5) (2006) 542-553.

[24] J. Hu, Z. Ge, K. Wang, Influence of cement fineness and water-to-cement ratio on mortar early-age heat of hydration and set times, Constr. Build Mater. 50 (2014) 657-663.

[25] ASTM, Standard Test Methods for Time of Setting of Hydraulic Cement by Vicat Needle, ASTM C191, ASTM International, West Conshohocken, PA, 2018.

[26] I.A. Pantazopoulos, I.N. Markou, D.N. Christodoulou, A.I. Droudakis, D.K. Atmatzidis, S.K. Antiohos, E. Chaniotakis, Development of microfine cement grouts by pulverizing ordinary cements, Cem. Concr. Compos. 34(5) (2012) 593-603.

[27] G. Sant, C.F. Ferraris, J. Weiss, Rheological properties of cement pastes: A discussion of structure formation and mechanical property development, Cem. Concr. Res. 38(11) (2008) 1286-1296.

[28] C.-L. Hwang, D.-H. Vo, V.-A. Tran, M.D. Yehualaw, Effect of high MgO content on the performance of alkali-activated fine slag under water and air curing conditions, Constr. Build Mater. 186 (2018) 503-513.

[29] ASTM, Standard Test Method for Measurement of Heat of Hydration of Hydraulic Cementitious Materials Using Isothermal Conduction Calorimetry, ASTM C1702, ASTM International, West Conshohocken, PA, 2017.

[30] K. Scrivener, R. Snellings, B. Lothenbach, A Practical Guide to Microstructural Analysis of Cementitious Materials, CRC Press, Landon, 2016.

[31] ASTM, Standard Test Method for Expansion and Bleeding of Freshly Mixed Grouts for Preplaced-Aggregate Concrete in the Laboratory, ASTM C940, ASTM International, West Conshohocken, PA, 2016.

[32] M.R. Azadi, A. Taghichian, A. Taheri, Optimization of cement-based grouts using chemical additives, J. Rock Mech. Geotech. Eng. 9(4) (2017) 623-637.

[33] H.N. Marsh, Properties and Treatment of Rotary Mud, SPE-931234-G 92(01) (1931) 234-251.

[34] M.J. Pitt, The Marsh Funnel and Drilling Fluid Viscosity: A New Equation for Field Use, SPE-62020-PA 15(01) (2000) 3-6.

[35] ASTM, Standard Test Method for Marsh Funnel Viscosity of Construction Slurries, ASTM D6910, ASTM International, West Conshohocken, PA, 2009.

[36] ASTM, Standard Test Method for Measuring Changes in Height of Cylindrical Specimens of Hydraulic-Cement Grout, ASTM C1090/C1090M, ASTM International, West Conshohocken, PA, 2015.

[37] I.D. Varga, B.A. Graybeal, Dimensional stability of grout-type materials used as connections between prefabricated concrete elements, J. Mater. Civ. Eng. 27(9) (2015) 04014246.

[38] C. Shi, D. Roy, P. Krivenko, Alkali-Activated Cements and Concretes, CRC Press, London, 2003.

[39] C. Shi, R.L. Day, A calorimetric study of early hydration of alkali-slag cements, Cem. Concr. Res. 25(6) (1995) 1333-1346.

[40] D.E. Giles, I.M. Ritchie, B.A. Xu, The kinetics of dissolution of slaked lime, Hydrometallurgy 32(1) (1993) 119-128.

[41] H. Khatami, B.C. O'Kelly, Prevention of bleeding of particulate grouts using biopolymers, Constr. Build Mater. 192 (2018) 202-209.

[42] A. Radocea, A new method for studying bleeding of cement paste, Cem. Concr. Res. 22(5) (1992) 855-868.

[43] L. Arenzana, R.J. Krizek, S.F. Pepper, Injection of dilute microfine cement suspensions into fine sands, Proceedings of the 12th International Conference on Soil Mechanics and Foundation Engineering, A.A. Balkema, Rio de Janeiro, Br, 1989, p. 4.

[44] F.T. Olorunsogo, Particle size distribution of GGBS and bleeding characteristics of slag cement mortars, Cem. Concr. Res. 28(6) (1998) 907-919.

[45] P.J. Wainwright, H. Ait-Aider, The influence of cement source and slag additions on the bleeding of concrete, Cem. Concr. Res. 25(7) (1995) 1445-1456.

[46] E. Nonveiller, Grouting Theory and Practice, Elsevier Science1989.

[47] X.M. Zhou, J.R. Slater, S.E. Wavell, O. Oladiran, Effects of PFA and GGBS on Early-ages engineering properties of portland cement systems, J. Adv. Concr. Tech. 10(2) (2012) 74-85.

[48] H. Beushausen, M. Alexander, Y. Ballim, Early-age properties, strength development and heat of hydration of concrete containing various South African slags at different replacement ratios, Constr. Build Mater. 29 (2012) 533-540.

[49] J.J. Brooks, M.A. Megat Johari, M. Mazloom, Effect of admixtures on the setting times of high-strength concrete, Cem. Concr. Compos. 22(4) (2000) 293-301.

[50] J.J. Chang, A study on the setting characteristics of sodium silicate-activated slag pastes, Cem. Concr. Res. 33(7) (2003) 1005-1011.

[51] T.A. Bier, F. Estienne, L. Amathieu, Shrinkage and shrinkage compensation in binders containing calcium aluminate cement, CAC: calcium aluminate cements 2001 (Edinburgh, 16-19 July 2001), 2001, pp. 215-226.

[52] S. Chatterji, Mechanism of expansion of concrete due to the presence of dead-burnt CaO and MgO, Cem. Concr. Res. 25(1) (1995) 51-56.

[53] Geo-Institute/ASCE, Jet Grouting Guideline, American Society of Civil Engineers, Reston, VA, 2009.

[54] M. Bruce, R. Berg, J. Collin, G. Filz, M. Terashi, D. Yang, Federal Highway Administration Design Manual: Deep Mixing for Embankment and Foundation Support, FHWA-HRT-13-046, US Department of Transportation, Federal Highway Administration, McLean, VA, 2013.

[55] M. Kitazume, M. Terashi, The Deep Mixing Method, CRC Press/Balkema, Leiden, Netherlands, 2013.

[56] S. Littlejohn, The development of practice in permeation and compensation grouting: A historical review (1802-2002): Part 1 Permeation grouting, Proceedings of the 3rd International Conference on Grouting and Ground Treatment, ASCE Geotech SP 120, 2003, pp. 50–99.

[57] J.K. Mitchell, In-place treatment of foundation soils, J. Soil Mech. Found. Div. 96(1) (1970) 73-110.

[58] E. Burwell, Cement and clay grouting of foundations: practice of the corps of engineers, J. Soil Mech. Found. Div. 84(1) (1958) 1-22.

[59] S. Zebovitz, R.J. Krizek, D.K. Atmatzidis, Injection of fine sands with very fine cement grout, J. Geotech. Eng. 115(12) (1989) 1717-1733.

[60] J.-S. Kim, I.-M. Lee, J.-H. Jang, H. Choi, Groutability of cement-based grout with consideration of viscosity and filtration phenomenon, Int. J. Numer. Anal. Meth. Geomech. 33(16) (2009) 1771-1797.

[61] S. Akbulut, A. Saglamer, Estimating the groutability of granular soils: a new approach, Tunn. Undergr. Space Technol. 17(4) (2002) 371-380.

[62] Y. Yi, L. Gu, S. Liu, F. Jin, Magnesia reactivity on activating efficacy for ground granulated blastfurnace slag for soft clay stabilisation, Appl. Clay Sci. 126 (2016) 57-62.